Chapter 4. Results and Discussions

4.1. Single-phase method for the synthesis of nanozeolites in organic medium

It is well known that in aqueous medium, zeolite precursors tend to aggregate during the crystallization, leading to the formation of undesired large zeolite crystals. To obtain small and uniform nanozeolites, in this study, an organic solvent is used as an alternative reaction medium for the hydrothermal treatment of organosilane-functionalized zeolite precursors. Typically, a clear aqueous zeolite gel solution and an organic solvent containing organosilane are mixed and heated with stirring at desired temperature for 12 h. Upon reacting with organosilane, the resulting zeolite precursors become hydrophobic and could enter and disperse in the organic phase. In this synthesis, the organic phase is a solution of toluene containing n-butanol; toluene is a suitable medium for the modification of zeolite with organosilane [22,134] and n-butanol acts as a surfactant [119,135]. After 6-12 hours of treatment, a clear mixture with only one phase was observed. This mixture was transferred into an autoclave for hydrothermal crystallization. The dispersion of functionalized zeolite precursors into the organic phase allows preventing these particles from growing during crystallization, thus resulting in small uniform nanocrystals.

The XRD pattern of the nanosilicalite-1 synthesized using this single-phase method at 170 ^{o}C for 24 h is shown in Figure 4.1.b. The XRD pattern of the large crystals prepared from the same zeolite gel solution in aqueous solution without organosilane (conventional method) is used as a reference (Figure 4.1.a). The XRD pattern of the sample is identical to that of the reference, indicating the MFI structure of the sample. There is a clear broadening of the reflections from the sample, which is attributed to small crystals. Furthermore, the sample is highly crystalline, i.e., the XRD pattern of this sample does not appear to contain a broad feature around $2\theta = 20\text{-}30^{\circ}$ which is characteristic of amorphous SiO_2 phase.

The XRD pattern of the as made FAU sample synthesized at 150 °C for 3 days using the same method is shown in Figure 4.2. This pattern is similar to that of samples prepared from the same zeolite gel solution using conventional method, implying the FAU structure. The fact that the peaks are broadened indicates the small size of the crystals.

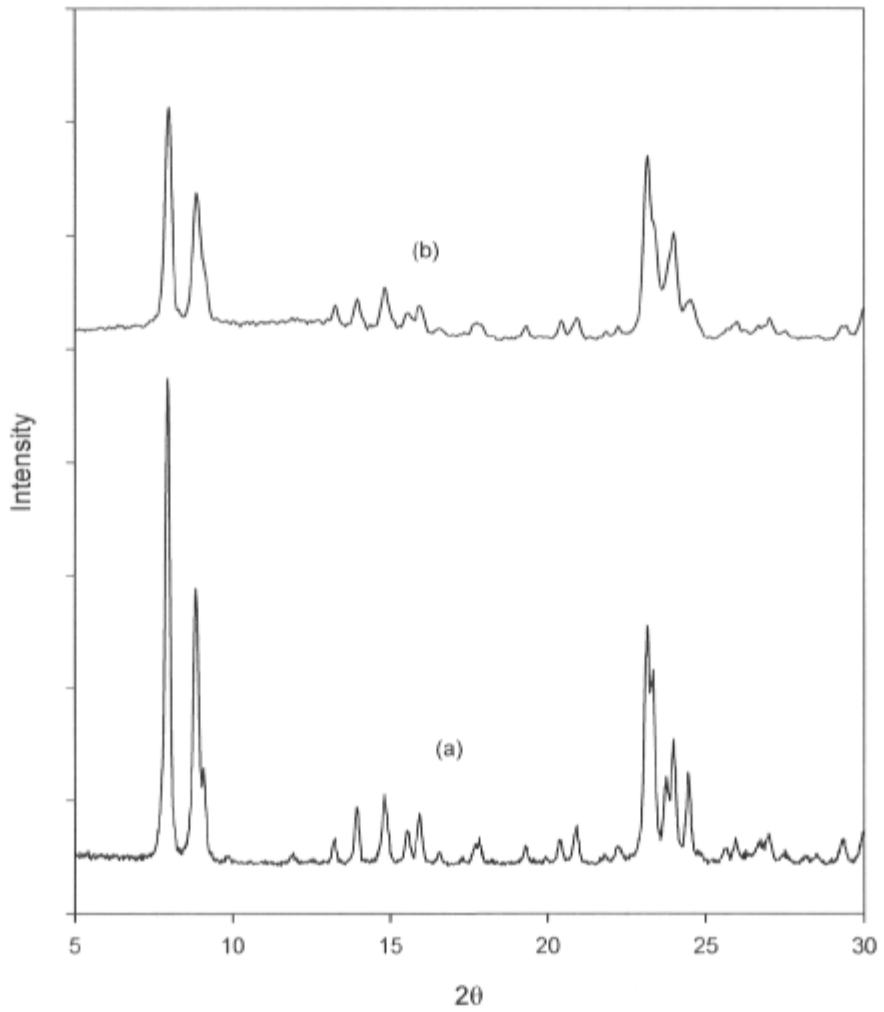

Figure 4.1. XRD patterns of the as made silicalite-1 samples prepared from the same synthesis solution (a) in aqueous solution using the conventional method: in absence of organosilane, (b) in solvent medium (phase): in the presence of organosilane

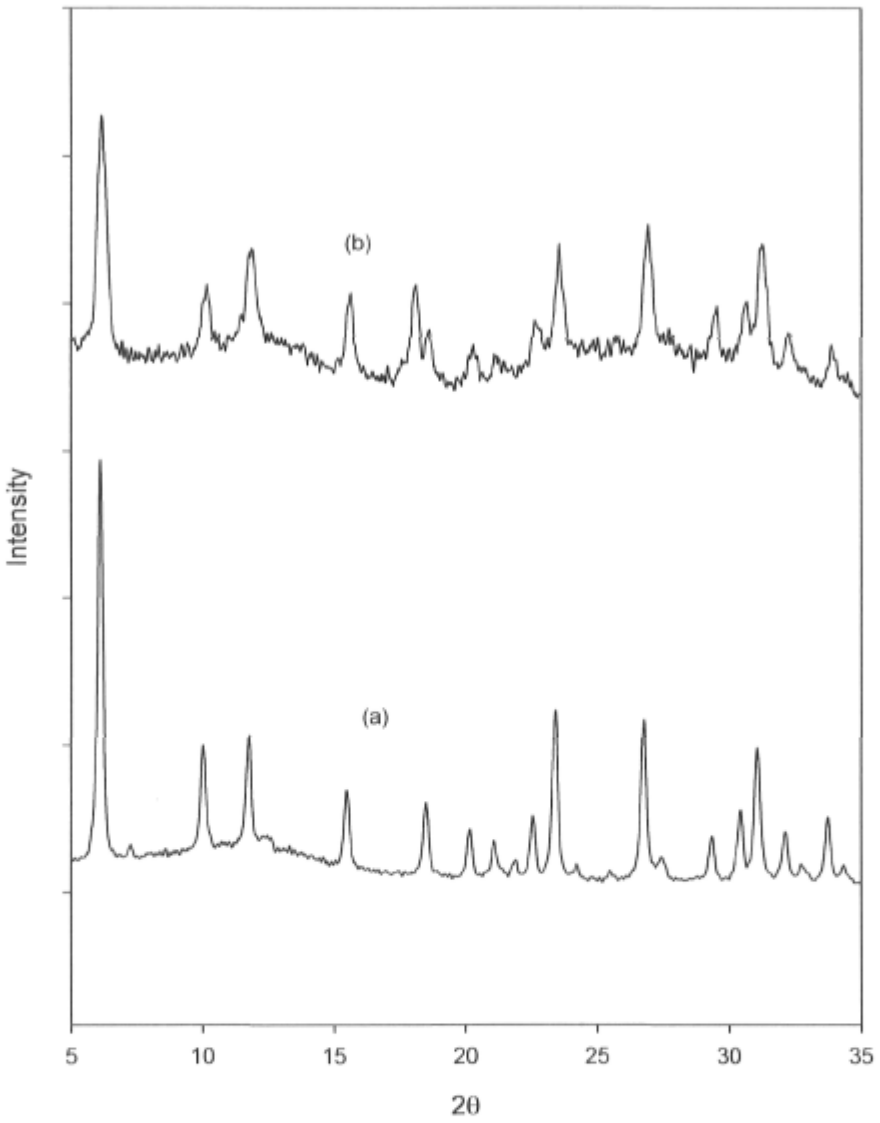

Figure 4.2. XRD patterns of the as made FAU zeolite samples prepared from the same synthesis solution (a) in aqueous solution using the conventional method: in absence of organosilane, (b) in solvent medium (phase): in the presence of organosilane

In order to establish the crystal size of the zeolite samples, the transmission electron micrographs (TEM) technique was used. A representative micrograph of the as made nanosilicalite-1 sample is shown in Figure 4.3. A small average crystal size of about 20 nm was observed. It is also seen that the crystal size distribution appears very uniform. This is expected since the precursors are protected from aggregation during the crystallization.

Figure 4.4 shows the TEM image of the FAU nanozeolite sample. The image of this sample clearly indicates highly crystalline nanozeolites with uniform size of 30 nm.

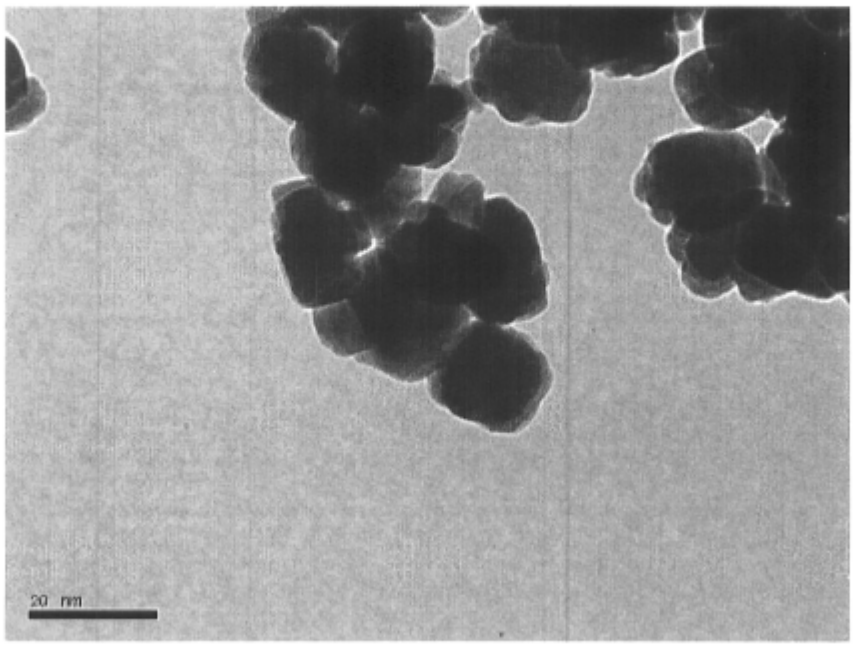

Figure 4.3. TEM micrograph of as-made nanosilicalite-1 prepared using the single-phase method

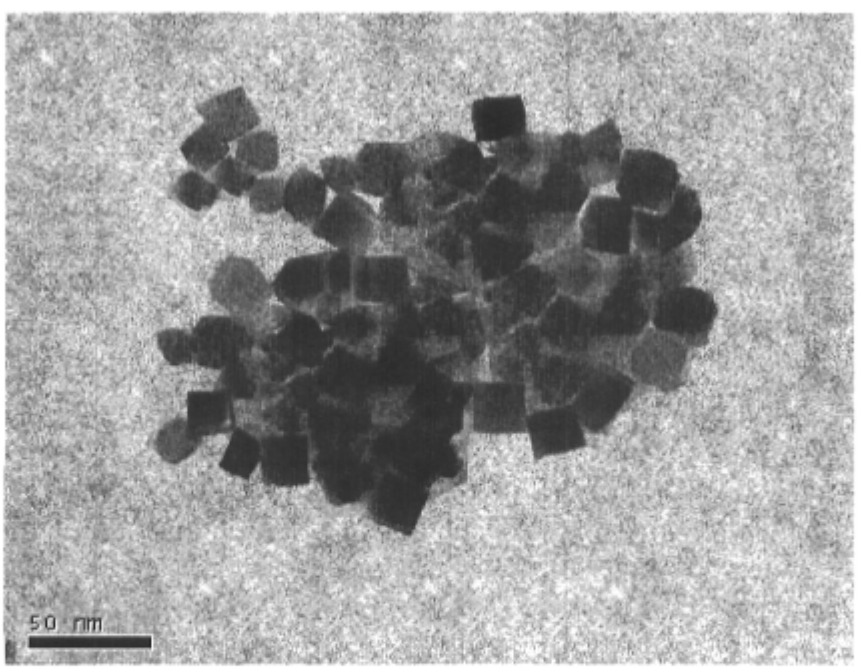

Figure 4.4. TEM micrograph of as made FAU nanozeolite prepared using the single-phase method

The FTIR spectra of as made nanosilicalite-1 prepared at different crystallization temperatures for 24 h are shown in Figure 4.5. It is observed in the spectrum of the product crystallized at 170 °C (Figure 4.5.a) that, the height and peak positions are identical to those of MFI structure. The peak at 450 cm^{-1} is assigned to the structure insensitive internal TO_4 (T = Si or Al). The peak around 550 cm^{-1} is attributed to the vibration of double 5-membered ring in MFI lattice. However, two adjacent peaks (544 and 555 cm^{-1}) are observed. According to [97] the presence of these two peaks indicates the formation of nanozeolites. The peak at 790 cm^{-1} is assigned to external linkage symmetric stretching. The peaks at 1080 and 1220 cm^{-1} are assigned to internal tetrahedral asymmetrical stretching and external linkage asymmetrical stretching respectively. It should be noted that the intensity of peak at 970 cm^{-1} attributed to the vibration of the external silanol groups is very low. This suggests that most of the external silanol groups have been functionalized with the organosilane. As the crystallization temperature decreases (Figure 4.5 b and c), however, the shape and height of the peak at 550 cm^{-1} which is sensitive to the MFI structure, are reduced. This observation suggests that, at lower temperature (less than 170 °C), under the same conditions, not all the precursors have been converted to zeolites.

The same trend is also observed in the synthesis of FAU nanozeolites. The FTIR spectra for the as made FAU nanozeolite samples synthesized at different temperatures are shown in Figure 4.6. The spectrum of the sample synthesized at 150 °C for 3 days is similar to that of the FAU structure. The peak at 460 cm^{-1} is assigned to the structure insensitive internal TO_4 (T = Si or Al) tetrahedral bending peak of zeolite Y. The peak at 565 cm^{-1} is attributed to the double ring external linkage peak assigned to zeolite Y. The peaks at 685 and 775 cm^{-1} are assigned to external linkage symmetrical stretching and internal tetrahedral symmetrical stretching respectively. Furthermore, the peaks at 1010 and 1080 cm^{-1} are assigned to internal tetrahedral asymmetrical stretching and external linkage asymmetrical stretching respectively. Overall, the FT-IR spectrum of this sample matches well with the typical FTIR absorption peaks of zeolite Y. However, for the sample prepared at lower temperature, at 100 °C, the height and shape peaks are lower, implying the low crystallinity of the sample.

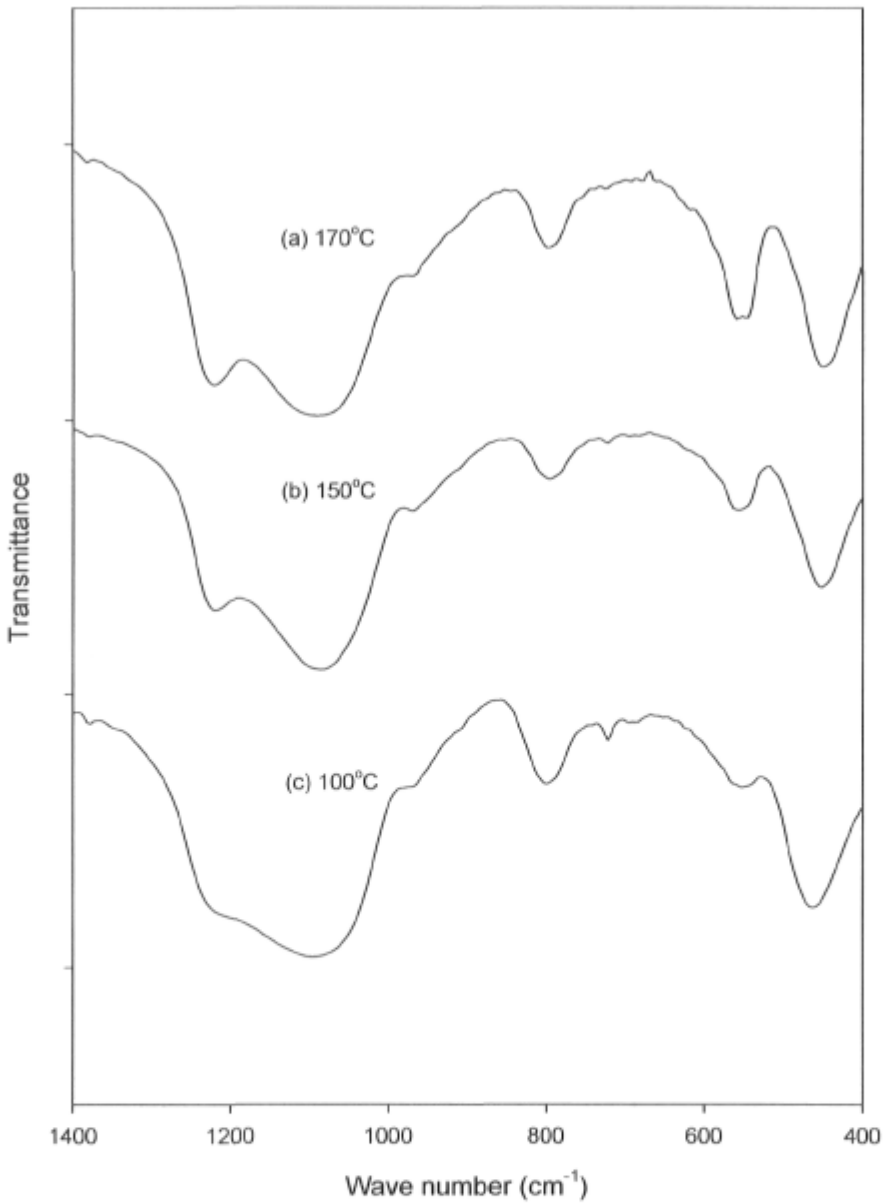

Figure 4.5. FTIR spectra of as made nanosilicalite-1 samples crystallized at different temperatures for 24 h: (a) 170 °C, (b) 150 °C, and (c) 100 °C

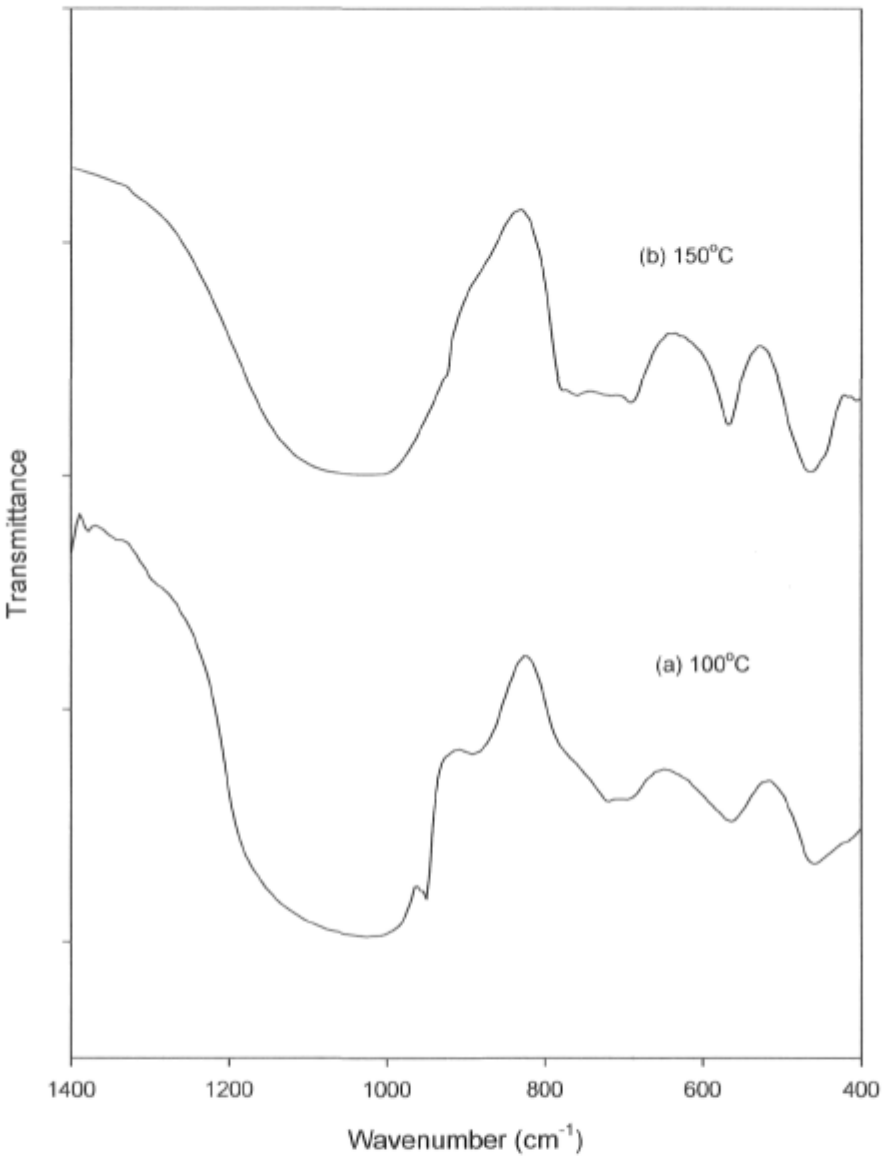

Figure 4.6: FTIR spectra of FAU samples synthesized at different temperatures: (a) 100 °C and (b) 150 °C

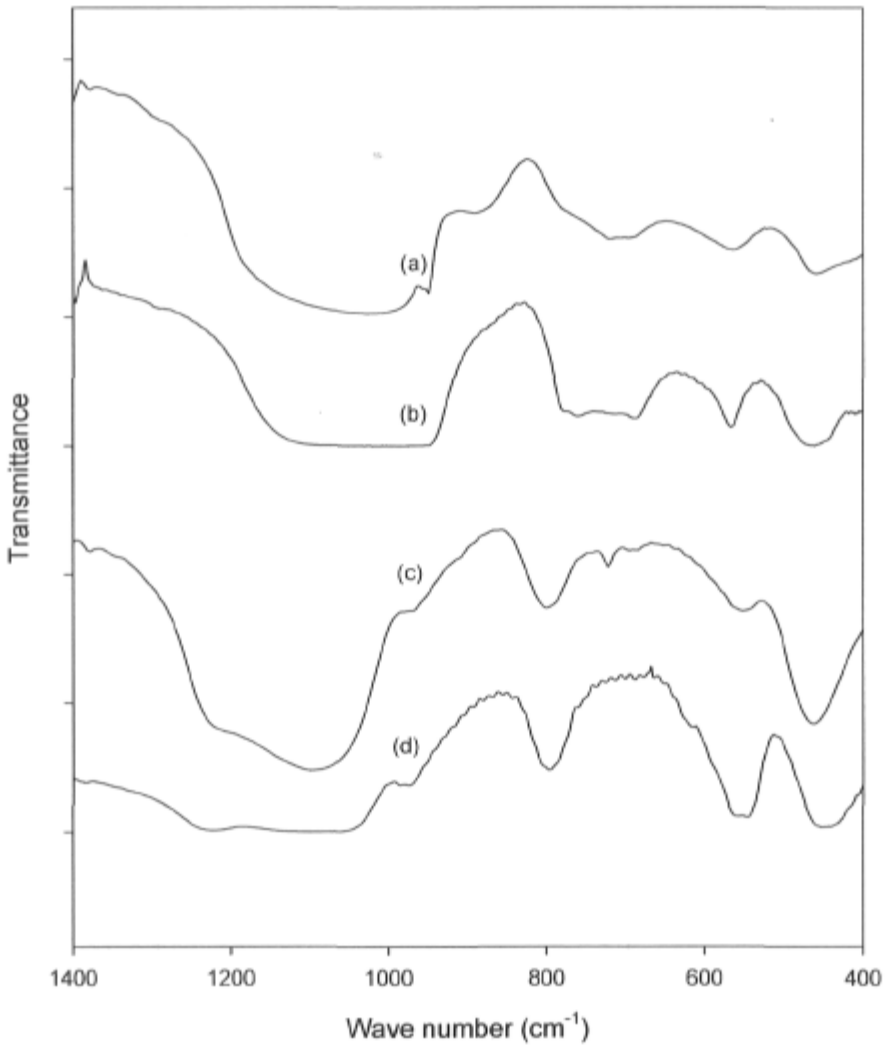

Figure 4.7. FTIR spectra of as made nanozeolites prepared using different methods under the same crystallization conditions: (a) and (c) FAU and silicalite-1, respectively prepared using the single-phase method, (b) and (d) FAU and silicalite-1, respectively prepared using the conventional method

For comparison, the synthesis of FAU and silicalite-1 using conventional method was also carried out. The crystallization conditions were similar to those of the single phase synthesis in organic medium, i.e. FAU zeolite was crystallized at 100 ^{o}C for 3 days, while nanosilicalite-1 was prepared at 100 ^{o}C for 1 day. The FTIR spectra of these FAU and silicalite-1 samples prepared using conventional method and single-phase method are

shown in Figure 4.7. In the spectra of the samples prepared using the single-phase method, the peak at 550-570 cm^{-1} which is attributed to the zeolite structure is lower as compared to that of the samples prepared using the conventional method. This observation suggests the higher crystallinity of the conventional samples.

Thus, it can be concluded that, the synthesis of nanozeolites using organic medium requires touch conditions compared with the conventional synthesis. It is likely that, the formation of zeolite structure in organic medium in the presence of organosilane is less favored than that in the aqueous phase. Hence, to obtain high crystallinity, higher crystallization temperature should be applied in this new method of synthesis.

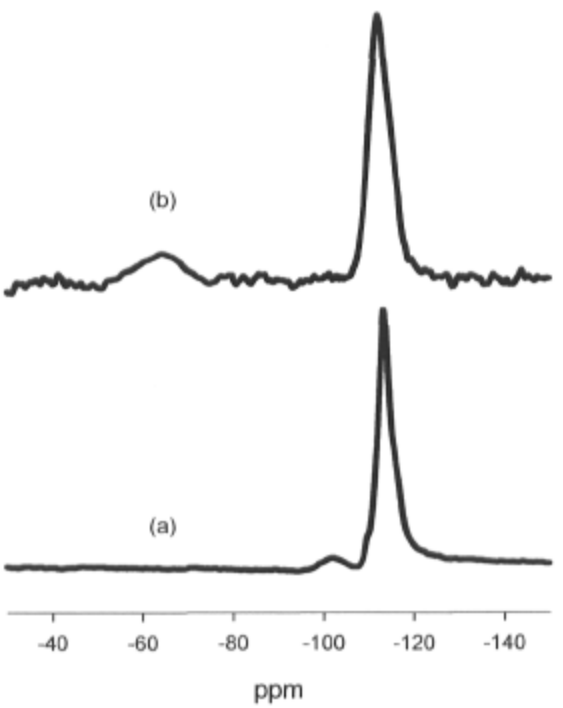

Figure 4.8. ^{29}Si NMR of the as made nanosilicalite-1 samples prepared from the same synthesis solution using different methods: (a) conventional method in aqueous medium without organosilane and (b) single phase method in organic solvent

The ^{29}Si MAS NMR technique was used to monitor the functionalization of the silanol groups on the surface of the zeolite nanocrystals. The ^{29}Si MAS NMR spectroscopy was carried out on dried samples (before calcination). The ^{29}Si MAS NMR spectroscopy of zeolites synthezed using the conventional method was also performed for comparison.

Figure 4.8 shows the NMR spectra of nanosilicalite-1 samples prepared using conventional (a) and the single-phase (b) method. For sample (a) two peaks at 110 ppm and 105 ppm which are characteristic of Q^4 ($Si(OSi)_4$) and Q^3 ($HOSi(OSi)_3$), respectively [97] were observed. However, for the sample (b) only one main peak at approximately 110 ppm which is assigned to Q^4 ($Si(OSi)_4$) was observed. In addition, a new peak at -68 ppm is present and is assigned to R-C-Si-$(OSi)_3$ species [136], the latter is the result from the reaction between the silicon in the organosilane and the surface silanol groups during the zeolite synthesis. Hence the NMR result has also confirmed the silylating reaction on the external surface of nanosilicalites-1.

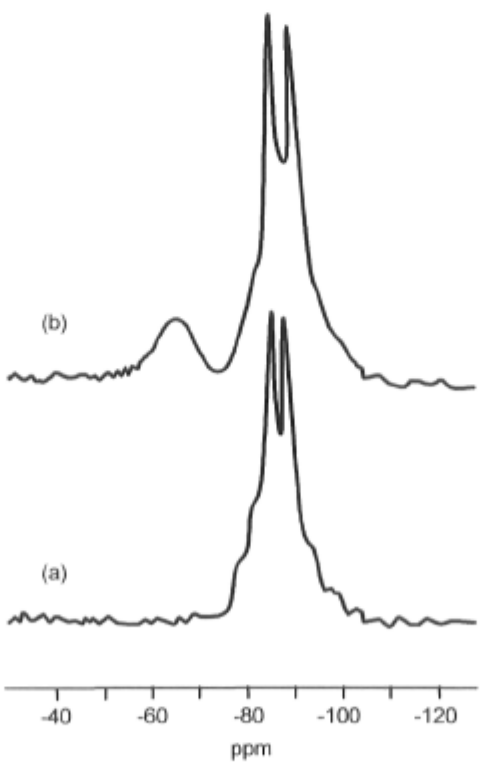

Figure 4.9. ^{29}Si NMR of the as made FAU nanozeolite samples prepared from the same synthesis solution using different methods: (a) conventional method and (b) single phase method in organic solvent

The ^{29}Si NMR spectra of the FAU nanozeolite and reference samples are shown in Figure 4.9. The presence of Q^4 species is observed at -103 ppm ($Si(OSi)_4$), - 98 ppm ($(OAl)(OSi)_3$), -94 ppm ($(OAl)_2(OSi)_2$), and at -84 ppm $Si(OAl)_4$. The peak at -68 ppm which is attributed to the C-$Si(OSi)_3$ was also observed. Hence it can be concluded that the FAU nanozeolites sample has been functionalized with the organosilane [136].

It is remarkable that the presence of Q^3 species was not detected in the NMR spectrum of the functionalized nanosilicalite-1 samples. However, for the silicalite reference sample prepared by the conventional method, the peak at about -100 ppm which is assigned to the silanol group $(SiO)_3OH$ was observed. This remark was also noticed in the spectrum of FAU nanozeolite as compared to that of the reference sample. In general, Q^3 species in FAU structure can be detected at -82.0 ppm ($Si(OAl)_3(OH)$), -87.0 ppm ($Si(OAl)_2(OSi)(OH)$), -92.8 ppm ($Si(OAl)(OSi)_2(OH)$), and -97.5 ppm ($Si(SiO)_3(OH)$. As seen in Figure 4.9, for the functionalized FAU nanozeolite sample, Q^4 signals became much broader with higher intensity as the Q^3 signals decrease, compared to those of the reference.

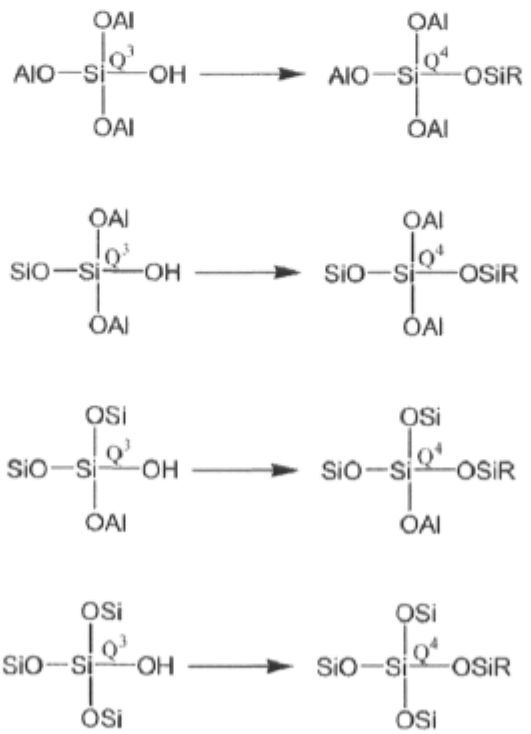

Figure 4.10. Schematic of transformation of Q^3 species to Q^4 [136]

This observation suggests that the protection of nanozeolites with organosilane led to the transformation of Q^3 species to Q^4. The nanozeolites became hydrophobic as the hydroxyl groups were replaced by the organic ones. The reactions are represented in Figure 4.10 [136].

Surface area and pore volume of nanozeolites were determined using nitrogen adsorption/desorption isotherms. Table 4.1 summarizes the physico-chemical properties of the series of zeolite samples prepared in solvent medium in presence of organosilane and prepared in aqueous medium in absence of organosilane. Figure 4.11 shows the typical N_2 adsorption/desorption isotherms and the modified BJH pore radius distribution of the nanosilicalite-1 sample synthesized using the two phase method. At low relative P/P_o pressure, a steep rise in uptake, followed by a flat curve, corresponds to filling of micropores with nitrogen. An inflection at higher pressures (e.g. in P/P_o range from 0.7-0.9) is characteristic of capillary condensation and is related to the range of mesopores. The specific surface area is 570 m^2/g and the external surface area based on t-plot calculation is 150 m^2/g. This high external surface value indicates the small crystal size of the sample.

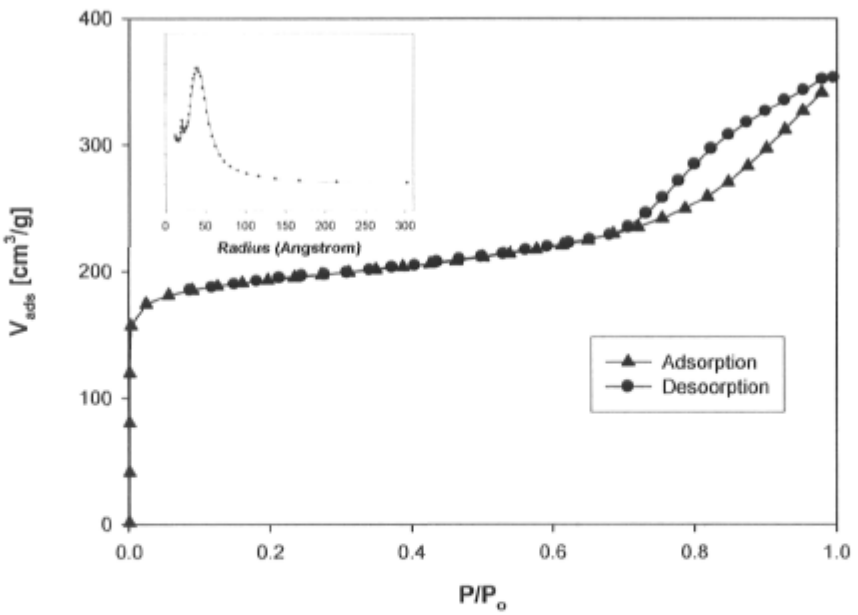

Figure 4.11. Nitrogen adsorption/desorption isotherms and BJH pore radius distribution of calcined nanosilicalite-1 prepared using the single phase method

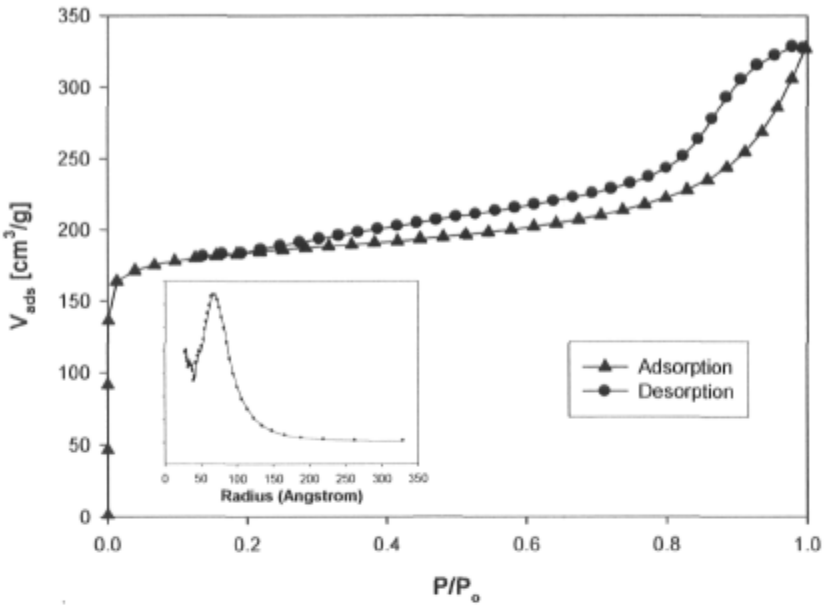

Figure 4.12. Nitrogen adsorption/desorption isotherms and BJH pore radius distribution of the calcined FAU sample synthesized using the single phase method

Table 4.1. Physicochemical properties of the calcined zeolite samples

Sample	S_{BET} (m^2/g)	S_{EXT} (m^2/g)	S_{MIC} (m^2/g)	V_{MIC} (cm^3/g)	R_{PORE} (nm)	Crystal size (nm)
Nanosilicalite-1	570	150	420	0.154	3.7	~20
Silicalite-1	512	15	479	0.162	-	~300
Nanofaujasite	545	96	449	0.149	6.5	~30
Faujasite	479	19	460	0.173	-	~400

Figure 4.12 also shows the nitrogen adsorption/desorption isotherms and the BJH pore radius distribution of the calcined FAU nanozeolite sample synthesized using the single phase method. The specific surface area of the sample is very high, e.g. 545 m^2/g. The external surface area is of high value of 96 m^2/g, which implies the presence of nanozeolites in the sample.

In conclusion, nanozeolites can be prepared using the single-phase synthesis method which allows producing uniformed and very small nanocrystals. The obtained products are protected with organosilane which in turn, brings about a hydrophobic character.

4.2. Two-phase method for the synthesis of nanozeolites in organic medium

The two-phase synthesis is an attractive method which has been used in the synthesis of inorganic nanoparticles such as Pt, TiO_2. CdS... [137-144]. In principle, the method employs both organic solvent and water as the reaction media. The formation of nanoparticles takes place at the interface between the two phases. If the organic solvent is previously added with some capping agent such as oleic acid or stearic acid, the resulting nanoparticles capped with these agents can be dispersed in the solvent. In this section we discus the adoption of the two-phase synthesis for the preparation of nanozeolites.

Since the crystallization of zeolites is somewhat different and difficult compared to the synthesis of conventional inorganic particles, care should be taken in choosing the appropriate "capping agent" and solvent for the synthesis of zeolites.

One of the problems in applying this method for the synthesis is that oxalic acid and stearic acid are incapable of "capping" zeolite crystals. In the synthesis of inorganic nanoparticles, these acids can attach to metal atoms by co-ordinate bonding. Thus, a transition metal atom which has an incomplete d sub-shell is more likely to form a complex with the acids compared to Si and Al atom in the structure of zeolites. Some surfactants such as CTAB, AOT can adsorb on the surface of zeolite crystals, however, the presence of these surfactants in the synthesis of zeolites has been reported to affect the morphology of the product as well as increase the crystal size [116-118].

This problem can be overcome by using organosilane as the protecting agent of zeolite nanocrystals. The aqueous solution of zeolite precursors was added with a solution of organosilane agent in an organic solvent. As the organic solvent is insoluble in water, the organic phase stays on top of the aqueous phase. Since the external surface of precursors is rich in silanol groups, they can react with the organosilane agents at the interface between

the two phases. The precursors hence are protected by organic groups which keep them from aggregation. Furthermore, because of the protecting organic groups, the precursors become more hydrophobic and can diffuse into the organic phase. Thus the growth stage is suppressed spatially in the two-phase synthesis.

To demonstrate this method, the synthesis of nanosilicalite-1 was carried out. The organosilane reagent used in this study was hexadecyltrimethoxysilane. This organosilane reagent was chosen because of its large molecular size so that the functionalization occurs only on the external surface. Toluene was chosen as the organic solvent since it can dissolve the organosilane [22,134]. After crystallization the products in the organic phase and aqueous phase were recovered separately by centrifugation and were denoted as OP and AP, respectively.

Figure 4.13 shows the X-ray powder pattern of the AP and OP samples. The XRD patterns of both samples are identical to that of the reference which was synthesized using the conventional method in aqueous solution in the absence of organosilane, indicating the MFI structure of the samples.

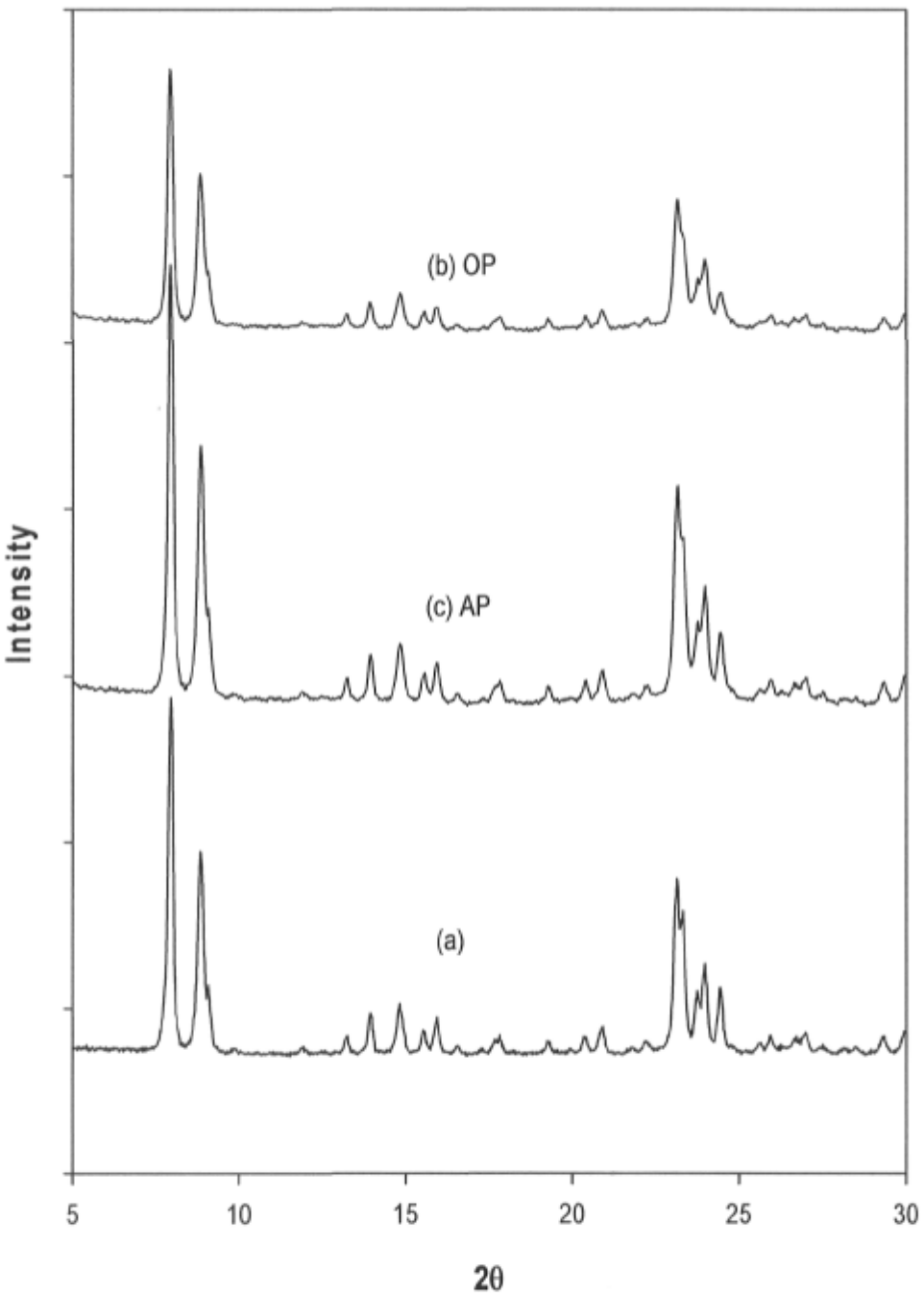

Figure 4.13. XRD patterns of the as made silicalite-1 samples, sample prepared using (a) conventional method in aqueous medium, (b) the two phase method, aqueous phase (AP), and (c) the two phase method, organic phase (OP)

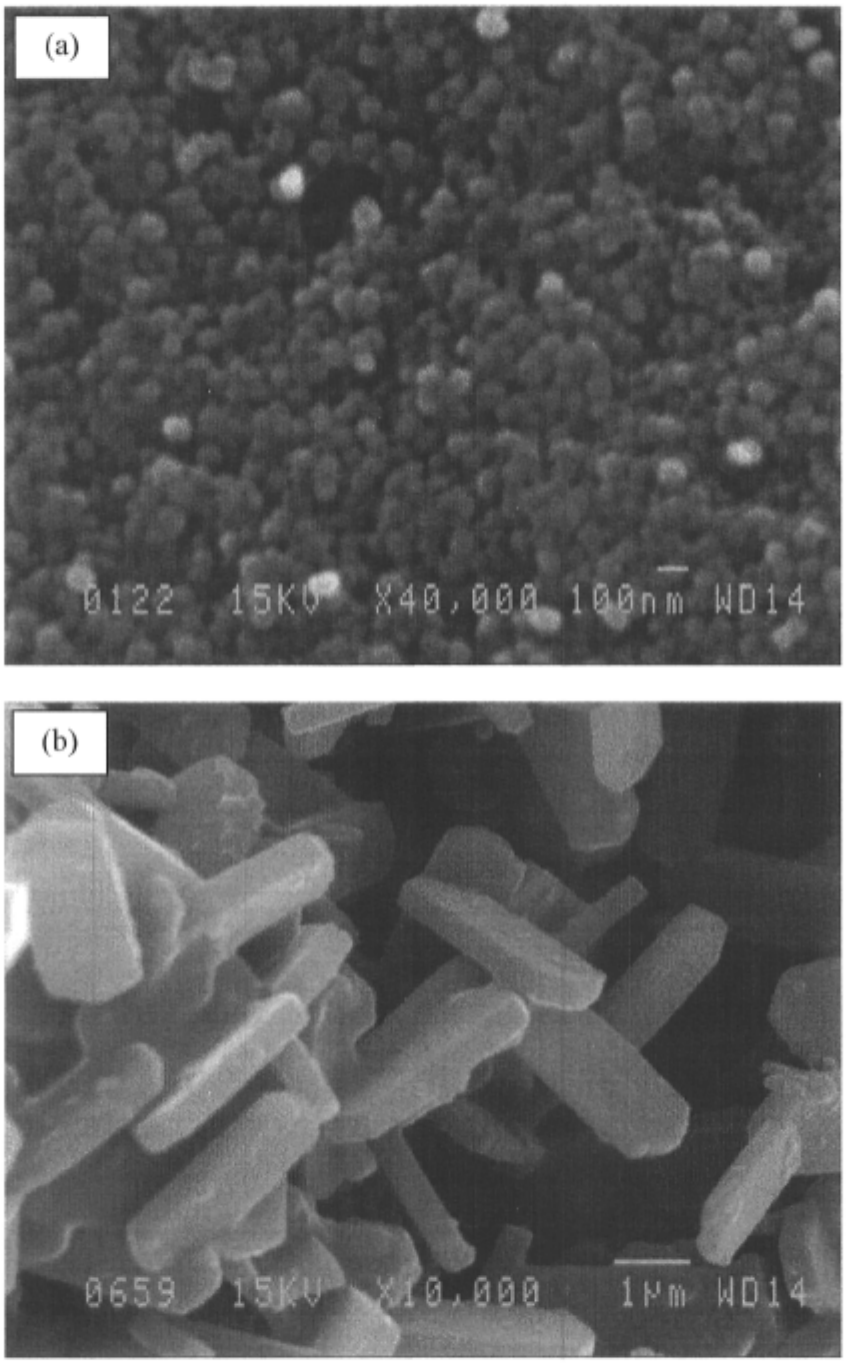

Figure 4.14. SEM micrographs of the as made silicalite-1 samples: (a) the two phase method, organic phase OP and (b) the two phase method, aqueous phase AP

The crystal size of the samples was investigated by the scanning electron microscope (SEM) technique. The crystal size of the OP sample was very small, ranging from 20 - 50nm. In contrast, large crystals of 5μm were observed in SEM micrograph of the AP sample. The difference between the two samples is interesting because it suggest the effect of the oganosilane agent on the crystal size of the product. Silanol sites on zeolites are located on the external surface and therefore the quantity of silanol sites is related to the zeolite crystal size. The large external surface of nanocrystalline zeolites provides significantly more silanol sites that are available for chemical functionalization than for zeolites with larger crystal sizes and smaller external surface areas. The nanocrystalline zeolites can be much more extensively functionalized than zeolites with larger crystal sizes. Therefore, only the functionalized nanozeolites were sufficiently hydrophobic to disperse into the organic phase whereas the large nanocrystals with lower degree of functionalization remained in the aqueous phase.

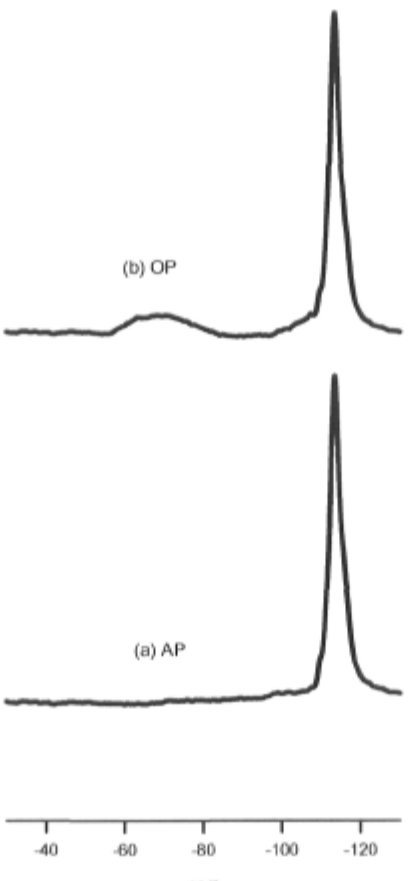

Figure 4.15. ^{29}Si MAS NMR spectra of the as made silicalite-1 samples: (a) AP and (b) OP

The ^{29}Si MAS NMR analysis of the dried AP and OP samples also confirmed this conclusion (Figure 4.15). The peaks at the range of 60 - 80 ppm, which indicates the presence of C-Si bond, were only found on the spectra of the OP sample.

As shown in Figure 4.16, the OP sample prepared from two-phase synthesis exhibits significant higher N_2 adsorption. The specific surface area is 520 m^2/g, the external surface area based on t-plot calculation is 106 m^2/g. This high external surface value indicates the small crystal size of the sample.

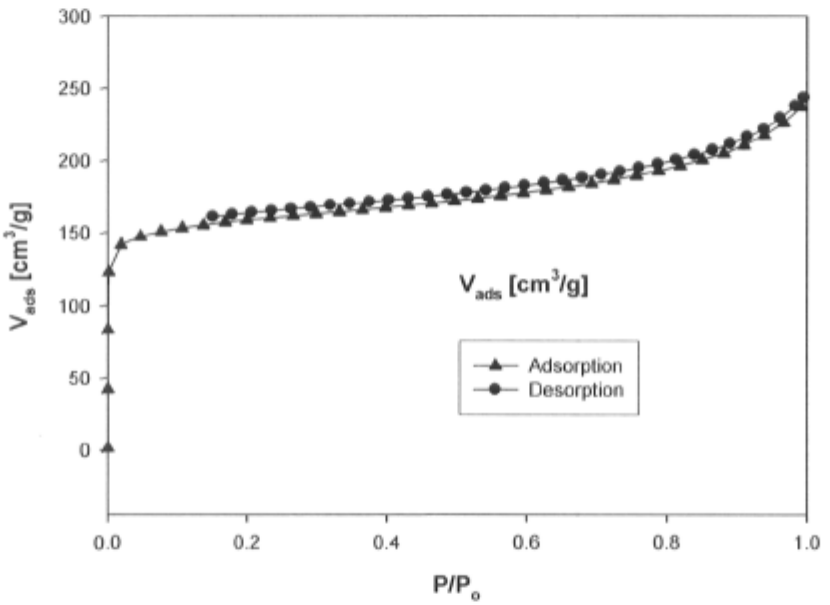

Figure 4.16. Nitrogen adsorption/desorption isotherms of the calcined nanosilicalite-1 OP sample

4.3. Characterization and activity of silica containing FAU nanozeolite in the cracking reaction of TIPB

4.3.1. Characterization

As mentioned in section 3.1.4 for the synthesis of the silica samples containing nanozeolite, the FTIR spectra of the nano-faujasite samples after calcination are shown in

Figure 4.17. All typical bands of the FAU structure are observed. This indicates that the FAU nanozeolite was stable at high temperature and the incorporation of silica did not lead to the destruction of the zeolite structure.

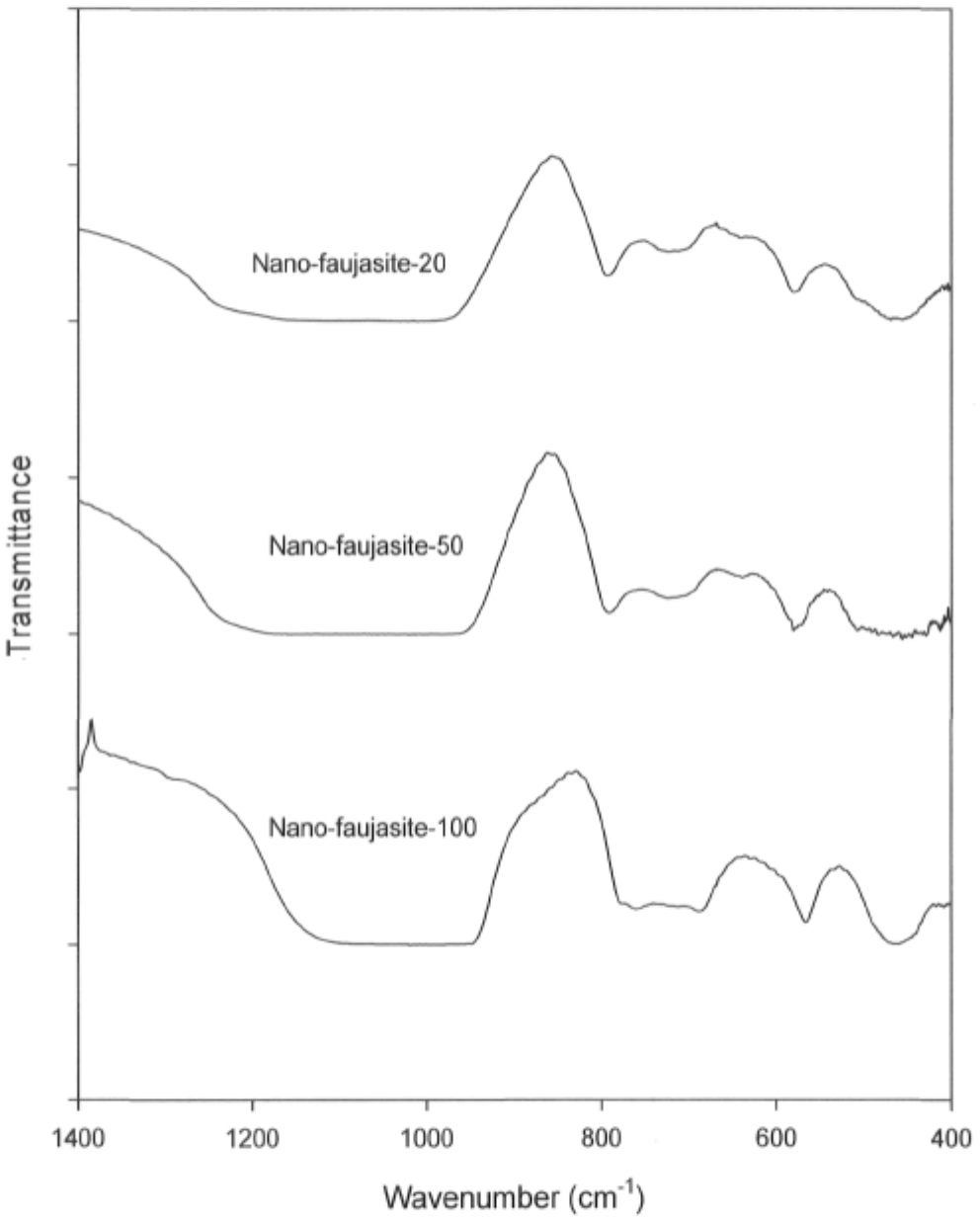

Figure 4.17. FTIR spectra of the calcined samples nano-faujasite-20, nano-faujasite-50 and nano-faujasite-100 (100% FAU nanozeolite content)

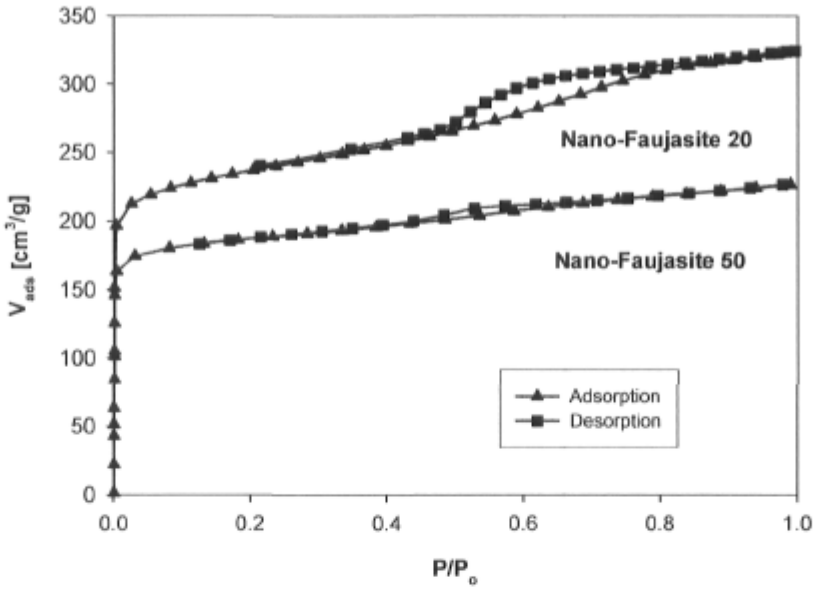

Figure 4.18. Nitrogen adsorption/desorption isotherms of nano-faujasite 20 and nano-faujasite 50 samples (spectra of nano-faujasite 20 is shifted by 50 a.u)

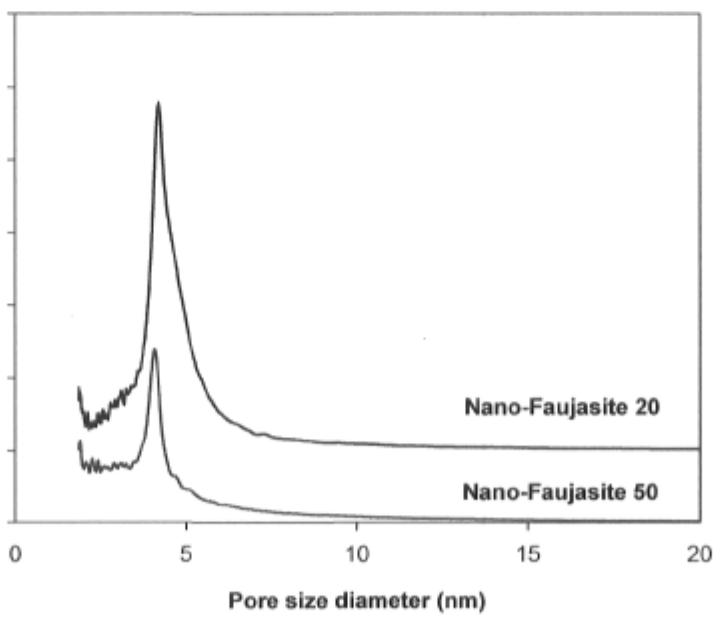

Figure 4.19. Pore size distributions of nano-faujasite 20 and nano-faujasite 50 samples (spectra of nano-faujasite 20 is shifted by 0.005 a.u)

Nitrogen adsorption/desorption isotherms and pore size distribution of the samples are shown in Figure 4.18 and Figure 4.19, respectively. The surface analysis results are summarized in Table 4.2. Given the specific surface area of FAU nanozeolite of 520 m^2/g, the incorporation of nanozeolites resulted in a significant increase in the surface areas of the resulting materials. Moreover, as the zeolite content increased the average pore size barely changed. This suggests that zeolite nanocrystals have been well dispersed in the mesoporous silica. There is no agglomeration inside the microporous silica which would lead to the decrease of the average pore size.

Table 4.2. Physicochemical properties of the calcined zeolite samples

Name	Nanozeolite content (%wt)	Si/Al (approximate)	BET surface area (m^2/g)	Average micropore diameter (Å)
Nano-Faujasite 20	20	20	610	42
Nano-Faujasite 50	50	10	600	40

4.3.2. Catalytic activity

The cracking reaction of TIPB is a useful probe reaction of examine the activity of external surface of the zeolite-based catalysis [145]. The reason is that TIPB molecules having a kinetic diameter of 0.9 nm are too big to access the internal surface of most types of zeolites. For example, TIPB molecules cannot pass through the pore mouth of FAU zeolites which is known to be about 0.74 nm as illustrated in Figure 4.20. Hence, any reactions of these molecules must occur only on the external surface of the zeolite. Nanozeolites with higher external surface are therefore expected to show higher activity than large zeolite crystals.

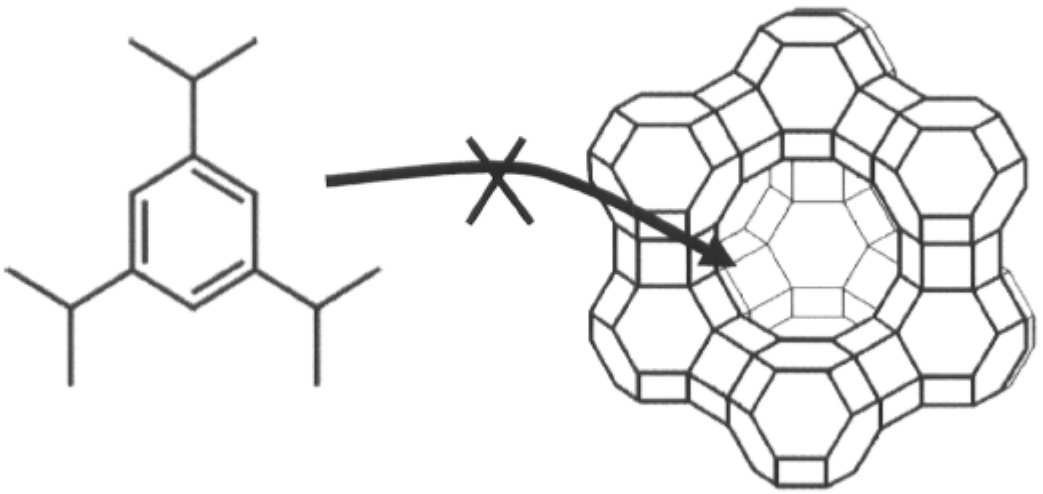

Figure 4.20. TIPB cannot disperse into the internal surface of FAU zeolites

The analysis of the cracking of TIPB over nano-faujasite catalysts are summarized in Table 4.3 and Table 4.4. For comparison, the reaction was also performed over the commercial FCC catalysts (Table 4.5). Both catalysts showed good activity. As the zeolite content in catalyst increased from 20%wt to 50%wt, the conversion shifted from 27.35% to 30.82%. The conversions over the two catalysts are even higher than commercial FCC catalyst which contained large zeolite crystals. The results suggests that external surface of nanozeolites dispersed in amorphous silica is accessible for the cracking reaction. The fact that high conversions were obtained on nano-faujasite samples is clear evidence that there is no detrimental effect on active sites of zeolite when the crystal size is reduced to the manometer domain. This conclusion is very important since it affords a possible approach to improve the activity of FCC catalyst by introduction of nanozeolites.

Table 4.3. Analysis of catalyst nano-faujasite-20 with TIPB model compound

Reactant	1,3,5-TIPB
Catalyst	M2
Cat/oil	5
mass of catalyst (g)	0.5
mass of reactant (g)	0.1

Run #	FID00410	FID00411	FID00412	FID00416	FID00417	FID00418	Average
Temperature (C)	530	530	530	530	530	530	530
Time (s)	5	5	5	5	5	5	5
Propene (propylene)	10.10	10.52	10.65	10.55	11.23	11.59	10.77333
Benzene	0.79	0.86	0.95	1.09	1.23	1.37	1.048333
Toluene	0.03	0.03	0.03	0.04	0.04	0.05	0.036667
Ethylbenzene	0.18	0.22	0.25	0.14	0.19	0.24	0.203333
p-m-xylene	0.07	0.07	0.06	0.09	0.08	0.09	0.076667
o-xylene	0.01	0.02	0.01	0.01	0.01	0.03	0.015
Ethenylbenzene (styrene)	0.01	0.02	0.01	0.01	0.01	0.04	0.016667
Isopropylbenzene (cumene)	5.58	5.42	5.28	5.90	5.84	5.82	5.64
n-propylbenzene	0.05	0.05	0.04	0.05	0.05	0.08	0.053333
1-methyl-4-isopropylbenzene (p-cymene)	0.00	0.01	0.01	0.00	0.00	0.02	0.008333
1,4-Diethylbenzene	0.24	0.37	0.37	0.26	0.42	0.50	0.36
1,3-Diethylbenzene	0.47	0.36	0.28	0.35	0.28	0.32	0.343333
1,2-DEB	0.04	0.04	0.03	0.02	0.02	0.06	0.035
1-methyl-4-isopropylbenzene	0.20	0.19	0.17	0.14	0.13	0.10	0.155
1,3-diisopropylbenzene	9.26	8.93	8.96	6.43	6.30	6.33	7.701667
1,4-DIPB	0.81	0.86	0.87	0.76	0.75	0.73	0.796667
1,3,5-TIPB	72.06	71.94	71.93	74.09	73.33	72.55	72.65
Conversion (%)	27.940	28.060	28.070	25.910	26.670	27.450	**27.35**

Table 4.4. Analysis of catalyst nano-faujasite-50 with TIPB model compound

Reactant	1,3,5-TIPB
Catalyst	M1
Cat/oil	5
mass of catalyst (g)	0.5
mass of reactant (g)	0.1

	Run #	FID00402	FID00403	FID00404	FID00405	FID00406	Average
	Temperature (C)	530	530	530	530	530	530
	Time (s)	5	5	5	5	5	5
Mass Fraction (%)	Propene (propylene)	16.04	16.10	12.99	14.25	14.86	14.848
	Benzene	1.58	1.66	2.39	2.73	3.01	2.274
	Toluene	0.03	0.03	0.04	0.05	0.05	0.04
	Ethylbenzene	0.32	0.35	0.18	0.22	0.25	0.264
	p-m-xylene	0.09	0.08	0.14	0.13	0.12	0.112
	o-xylene	0.02	0.02	0.01	0.01	0.01	0.014
	Ethenylbenzene (styrene)	0.02	0.02	0.01	0.03	0.03	0.022
	Isopropylbenzene (cumene)	5.51	5.51	6.66	6.71	6.66	6.21
	n-propylbenzene	0.04	0.04	0.06	0.06	0.06	0.052
	1-methyl-4-isopropylbenzene (p-cymene)	0.009	0.01	0.007	0.003	0.00	0.006
	1,4-Diethylbenzene	0.43	0.45	0.29	0.49	0.51	0.434
	1,3-Diethylbenzene	0.59	0.54	0.39	0.29	0.25	0.412
	1,2-DEB	0.02	0.02	0.02	0.02	0.02	0.02
	1-methyl-4-isopropylbenzene	0.11	0.10	0.13	0.11	0.10	0.11
	1,3-diisopropylbenzene	5.99	5.89	4.4	4.42	4.59	5.058
	1,4-DIPB	0.87	1.08	0.78	0.74	0.83	0.86
	1,3,5-TIPB	68.24	68.01	71.41	69.66	68.55	69.174
	Conversion (%)	31.760	31.990	28.590	30.340	31.450	**30.826**

Table 4.5. Conversion of 1,3,5-TIPB (triisopropylbenzene) over FCC commercial catalyst

Products	Run 1	Run 2	Run 3	Run 4	Run 5	Run 6	Average
Propylene	11.64	11.77	11.99	11.48	12.22	11.53	**11.77**
C3-C6							
Benzene	7.30	7.38	7.78	6.24	7.60	7.13	**7.24**
Toluene	0.27	0.27	0.29	0.21	0.28	0.25	**0.26**
Ethylbenzene	0.01	0.01	0.00	0.00	0.00	0.00	**0.00**
p-m-xylene	0.61	0.60	0.63	0.60	0.63	0.59	**0.61**
o-xylene	0.10	0.07	0.08	0.06	0.08	0.07	**0.08**
Ethenylbenzene	0.05	0.02	0.04	0.04	0.03	0.02	**0.03**
Isopropylbenzene	1.18	1.24	1.22	1.54	1.23	1.17	**1.26**
n-propylbenzene	0.36	0.35	0.35	0.33	0.35	0.34	**0.35**
1-methyl-4-isopropylbenzene	0.03	0.02	0.02	0.02	0.02	0.02	**0.02**
1,4 Diethylbenzene	0.08	0.05	0.06	0.09	0.07	0.05	**0.07**
1,3 Diethylbenzene	0.06	0.03	0.03	0.04	0.04	0.03	**0.04**
1,2 Diethylbenzene	0.05	0.03	0.02	0.05	0.04	0.03	**0.04**
1-methyl-4-isopropylbenzene	0.06	0.02	0.02	0.04	0.03	0.02	**0.03**
1,3-Diisopropylbenzene	0.65	0.67	0.60	0.66	0.69	0.69	**0.66**
1,4 Diisopropylbenzene	1.23	1.07	0.99	1.07	1.07	1.04	**1.08**
1,3,5-Triisopropylbenzene	76.21	76.32	75.80	77.46	75.55	76.92	**76.38**
Total Products	**99.89**	**99.92**	**99.92**	**99.93**	**99.93**	**99.90**	**99.92**
Coke (gr carbon/gr catalyst)*100 (%)	**0.11**	**0.11**	**0.11**	**0.11**	**0.11**	**0.11**	**0.11**
Conversion (without coke)	**23.79**	**23.68**	**24.20**	**22.54**	**24.45**		
Conversion (with coke)	**23.81**	**23.70**	**24.22**	**22.56**	**24.47**		
Average Conversion (without coke)							**23.62**
Average Conversion (with coke)							**23.64**